Technical University of Denmark

DTU

Deterministic superresolution with coherent states at the shot noise limit

Distante, Emanuele; Jezek, Miroslav; Andersen, Ulrik Lund

DTU Library
Technical Information Center of Denmark

PHYSICAL REVIEW LETTERS

Deterministic Superresolution with Coherent States at the Shot Noise Limit

Emanuele Distante,[1,2,*] Miroslav Ježek,[1,3] and Ulrik L. Andersen[1]

[1]*Department of Physics, Technical University of Denmark, Fysikvej, 2800 Kongens Lyngby, Denmark*
[2]*Dipartimento di Fisica, Universita degli Studi di Milano, I-20133 Milano, Italy*
[3]*Department of Optics, Faculty of Science, Palacký University, 17. listopadu 12, 77146 Olomouc, Czech Republic*
(Received 23 November 2012; published 17 July 2013)

Interference of light fields plays an important role in various high-precision measurement schemes. It has been shown that superresolving phase measurements beyond the standard coherent state limit can be obtained either by using maximally entangled multiparticle states of light or using complex detection approaches. Here we show that superresolving phase measurements at the shot noise limit can be achieved without resorting to nonclassical optical states or to low-efficiency detection processes. Using robust coherent states of light, high-efficiency homodyne detection, and a deterministic binarization processing technique, we show a narrowing of the interference fringes that scales with $1/\sqrt{N}$ where N is the mean number of photons of the coherent state. Experimentally we demonstrate a 12-fold narrowing at the shot noise limit.

When two coherent electromagnetic waves interfere, as in Young's double slit experiment or in a standard Mach-Zehnder interferometer, an oscillatory interference pattern arises with a periodicity governed by the wavelength, λ, of the field. The period is given by $\lambda/2$ and is often referred to as the standard resolution limit of interferometers (and in imaging it is the Rayleigh resolution criterion [1]). Superresolution–that is resolution beyond the standard $\lambda/2$ limit—can be attained by the use of quantum entanglement. For example, using the maximally path-entangled multiparticle NOON states, $|\text{NOON}\rangle = (|N0\rangle + |0N\rangle)/\sqrt{2}$, it is possible to achieve superresolution with resolvable features down to $\lambda/(2N)$ where N is the number of photons [2]. Superresolution with NOON states has been demonstrated with ions [3], nuclear spins [4], atoms [5], and photons [6–10]. In addition to superresolution, the NOON states can in principle also beat the quantum shot noise limit (SNL) in phase estimation ultimately reaching the optimal estimation known as the Heisenberg limit [11]. However, since these states are extremely fragile and are prepared and detected with very low efficiency [12], it is experimentally very challenging to beat the SNL [13,14]. Another approach to obtain superresolution and supersensitivity is to use single photons in a multiple-pass configuration [15,16].

Coherent states of light have also been used to obtain superresolution. The idea is to detect a nonclassical state (such as the NOON state) via state projection as opposed to nonclassical state preparation [17]. Examples of projections of coherent states that lead to phase superresolution are photon counting, coincidence counting, and parity detection [10,18–25]. Despite its superresolving capability, this state projection method cannot beat the SNL in phase estimation but it may approach it for an optimized parity detector [21,25]. Although this method

largely reduces the complexity of the preparation stage, the detection part remains complex (ideally requiring photon number resolving detectors) and the efficiency in projecting out the desired nonclassical state is often very low [20].

In this Letter we propose and demonstrate a simple and very efficient scheme to obtain superresolution at the SNL without the need of complex states in preparation or complex projectors in detection. We use coherent states of light and a simple high-efficiency homodyne detector to achieve phase superresolution beyond what has been achieved with any non-Gaussian resources or detectors. The method is deterministic and we show that it operates close to the shot noise limit in contrast to all previous implementations of coherent state based superresolution.

Our method follows the interferometric scheme illustrated in Fig. 1(a). A coherent state of light, $|\alpha\rangle$, with amplitude α and mean photon number $N = |\alpha|^2$ enters the interferometer at the input symmetric beam splitter. The resulting state, $|\alpha/\sqrt{2}\rangle|\alpha/\sqrt{2}\rangle$, acquires a phase shift, ϕ, in one arm of the interferometer, and the final state at the output, $|\Psi(\phi)\rangle = |\cos(\phi/2)\alpha\rangle|\sin(\phi/2)\alpha\rangle$, is produced by interference at the second beam splitter. The observed phase resolution and sensitivity crucially depend on how this output state is detected. By describing the detection process with a measurement operator $\hat{\Pi}$, the response function of the setup is the mean value of that operator, $\langle\hat{\Pi}\rangle$. Using, for example, a standard intensity detector described by the observable $\hat{\Pi} = \hat{N}$, the detector response is $N\cos^2(\phi/2)$ which is an oscillating function with a period given by $\lambda/2$, thus coinciding with the standard resolution limit. In the following we show that by substituting the intensity detector with a simple homodyne detector combined with a postbinarization process, we beat the standard resolution limit.

The main idea of our approach is to divide the quadrature measurement outcomes into two bins: Assuming that we measure the phase quadrature, $\hat{p}$ (where $\hat{p} = (\hat{a} - \hat{a}^\dagger)/2i$ and $\hat{a}$ is the field operator), we classify two different results associated with outcomes in the intervals $|p| \leq a$ and $|p| > a$. Such a measurement strategy is described by the two projectors

$$\hat{\Pi}_0 = \int_{-a}^{a} dp |p\rangle\langle p|, \qquad \hat{\Pi}_1 = \hat{I} - \hat{\Pi}_0, \qquad (1)$$

and the measurement observable can thus be written as $\hat{\Pi} = \lambda_0 \hat{\Pi}_0 + \lambda_1 \hat{\Pi}_1$ where $\lambda_0 = 1/\text{erf}(\sqrt{2}a)$ and $\lambda_1 = 0$ are the eigenvalues associated with the two measurement outcomes. These eigenvalues are found from the normalization with a vacuum state for $\hat{\Pi}_0$ and using $[x, p] = i/2$. The detector response function of this dichotomic strategy is

$$\langle \hat{\Pi} \rangle = \frac{1}{\text{erf}(\sqrt{2}a)} \int_{-a}^{a} dp |\langle \sqrt{N} \sin(\phi/2)|p\rangle|^2. \qquad (2)$$

For a general value of a the response function cannot be evaluated in closed form in terms of elementary functions but for $a \to 0$ (corresponding to binning the results for which $p = 0$ and $p \neq 0$), it can be simply written as

$$\langle \hat{\Pi} \rangle = \exp\left(-\frac{1}{2} N \sin^2 \phi\right) \qquad (3)$$

and is illustrated in Fig. 1(b). The full width at half maximum of this fringe is $\text{FWHM} = 2 \arcsin\sqrt{(2\ln 2)/N}$, and by comparing it to the FWHM of the fringe associated with a standard resolution limited intensity detection system, we see that superresolution is obtained for $N > 2 \ln 2$. For $N \to \infty$ we find a $1/\sqrt{N}$ improvement of the resolution with respect to the standard limit. We note that for $a \to 0$, one of the measurements is associated with the projection onto a state with an even photon number (infinitely squeezed state) which is somewhat reminiscent of one of the projectors of a parity measurement [21].

In addition to being superresolving, our approach also exhibits a phase sensitivity at the SNL. The sensitivity is defined as $\Delta\phi = \Delta\Pi/|d\langle\hat{\Pi}\rangle/d\phi|$ where $\Delta\Pi = \sqrt{\langle\hat{\Pi}^2\rangle - \langle\hat{\Pi}\rangle^2}$, and for our measurement operator (with $a \to 0$) it reaches the minimum value of

$$\Delta\phi_{\min} = \sqrt{\sqrt{\frac{\pi}{2}} \frac{e^{(1/4)(2+N-\sqrt{4+N^2})} - \sqrt{2/\pi}}{\sqrt{4+N^2} - 2}} \qquad (4)$$

near the phase points $\phi_{\min} = \pm \arccos(\sqrt{1/2} - 1/N + \sqrt{4+N^2}/2N)$ and for large N it converges to $\Delta\phi_{\min} = \sqrt{(\sqrt{e\pi/2} - 1)/N} \approx 1.03/\sqrt{N}$, thus being close to the SNL.

In the limit of $a \to 0$ the measurement is not physically sound as it requires infinitely high energy. However, both
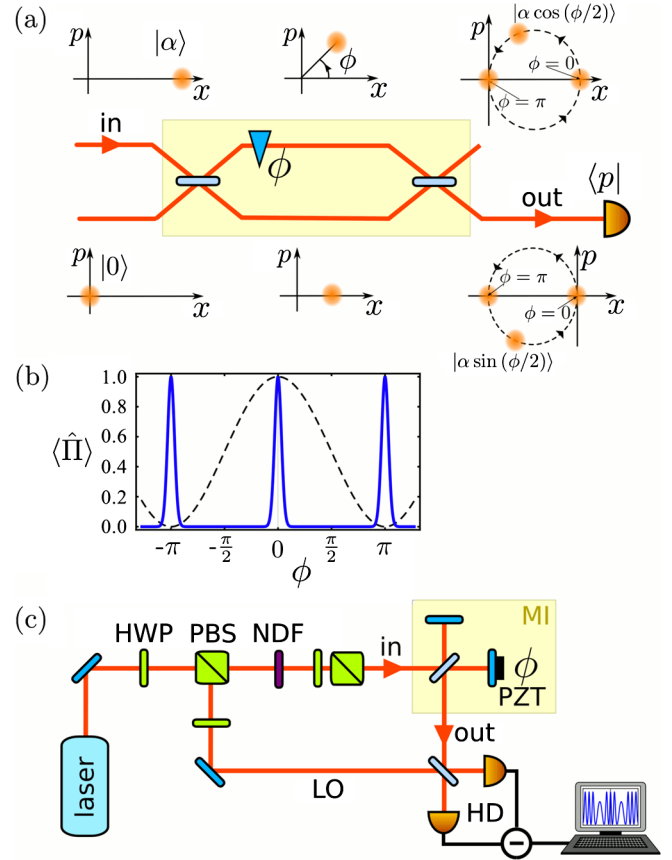

FIG. 1 (color online). Experimental setup and illustration of the principles. (a) Schematic of the experimental setup. A product of a coherent state, $|\alpha\rangle$, and a vacuum state, $|0\rangle$, is transformed through an interferometer and measured with a homodyne detector described by the ideal projector $\langle p|$. The evolutions in phase space of the two states are illustrated by the insets. (b) The phase response function $\langle\Pi\rangle$ for the standard interferometer scheme (dashed curve) and for the superresolving scheme (solid curve). (c) Experimental setup. Light from a picosecond pulsed Ti:sapphire laser operating at 830 nm and with a repetition rate of 800 kHz is controllably divided into two beams using a half-wave plate (HWP) and a polarizing beam splitter (PBS) thereby creating a signal and a local oscillator (LO) beam for homodyne detection (HD). The power of the signal beam is controlled by a neutral density filter (NDF), a HWP and a PBS, and subsequently sent into a Michelson interferometer (MI), the function of which is identical to the one in (a). A piezocrystal (PZT) attached to one of the interferometer mirrors scans the phase, ϕ, and the resulting output is measured by means of HD.

the resolution and sensitivity properties are preserved even for a finite value of a. Indeed, for a general value of a the response function can be evaluated as

$$\langle \hat{\Pi} \rangle = \frac{1}{2\text{erf}(\sqrt{2}a)} \{\text{erf}[\sqrt{2}g_+] + \text{erf}[\sqrt{2}g_-]\}, \qquad (5)$$

where $g_\pm = a \pm (1/2)\sqrt{N}\sin\phi$. The response function and its width is illustrated by the solid curves in
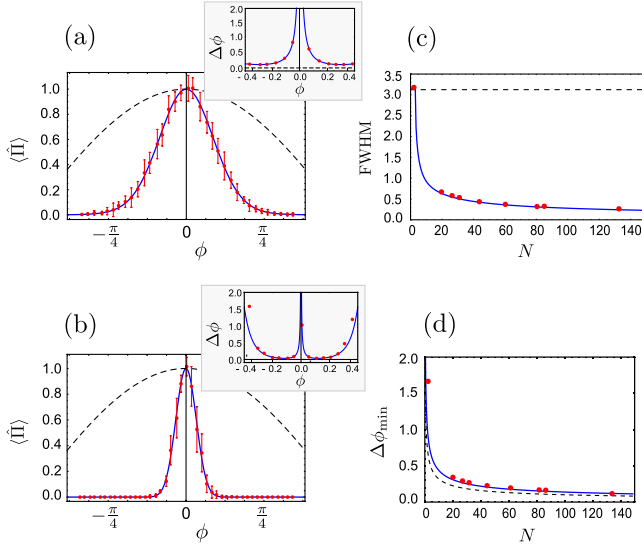
FIG. 2 (color online). Performance of the superresolving in-
terferometer. (a) and (b) show the experimental results (dots) and
the theory (solid curve) for the response function with $a = 0.5$
for two different mean photon numbers $N = 19$ and $N = 132$,
respectively. The dashed curves represent the standard Rayleigh
limited strategy. The insets of (a) and (b) are the results of the
sensitivity as a function of ϕ for the same values of N. The
dashed curves represent the SNL. (c) The resolution in terms of
FWHM of our scheme as a function of the mean photon number
(red dots) together with theory for our approach (solid curve) and
for Rayleigh limited strategy (dashed line). (d) Minimum value
of the sensitivity for our scheme for different mean photon
numbers (red dots). The solid curve represents the theoretical
curve, $\Delta\phi_{\min} \approx 1.37/\sqrt{N}$, and the dashed line stands for the
SNL. Error bars of (c), (d) and the insets are smaller than the
data points.

Figs. 2(a)–2(c). The scaling of the width is again found to
be $1/\sqrt{N}$. Finally, the sensitivity for a finite a reads

$$\Delta\phi = \sqrt{\frac{\pi}{2} \frac{e^{(2a+\sqrt{N}\sin\phi)^2}(2-k)k}{N\cos^2\phi(e^{4a\sqrt{N}\sin\phi} - 1)^2}} \quad (6)$$

where $k = \text{erfc}[\sqrt{2}g_-] + \text{erfc}[\sqrt{2}g_+]$ and $\text{erfc}(\cdots) = 1 -$
$\text{erf}(\cdots)$ is the complementary error function. For $a = 1/2$
and $N \gg 1$ the sensitivity follows the shot noise scaling;
$\Delta\phi_{\min} \approx (1.37/\sqrt{N})$. The value of $a = 1/2$ represents a
trade-off between sensitivity and resolution. For example,
for a higher value of a the sensitivity is closer to the SNL
but the resolution FWHM increases and vice versa.

We now implement the protocol using the setup dis-
played in Fig. 1(c). A coherent state with a controllable
mean photon number is sent through a Michelson interfer-
ometer (MI) in which the relative phase (ϕ) is continuously
varied by a piezodriven mirror. The phase quadrature of the
interferometer output state is then measured with a high-
efficiency homodyne detector (HD) with an overall effi-
ciency of 90% (stemming from a diode efficiency of 95%
and interference contrast of 98%). We subject the resulting

detector outcomes to the binning procedure with the inter-
val set to $a = 1/2$. The average photon number N is
estimated by directing the input signal (by-passing the
interferometer) to the homodyne detector and measuring
the amplitude, α of the state ($N = |\alpha|^2$). The reading is
calibrated against the vacuum trace (shot noise). The
experiment is repeated 400 times for each realization of a
phase value, and the frequencies at which the measurement
outcomes fall within the two quadrature intervals
[described by the projectors (1)] are found. The resulting
response functions are plotted in Figs. 2(a) and 2(b) for two
different power levels (red dots). A clear narrowing of the
fringe with respect to the fringe for the standard approach
(dashed curve) is observed, thus proving the superresolu-
tion capabilities of our scheme. We also note that the
visibility of the new interference fringes is basically
unchanged and close to unity. We repeat the experiment
for several different mean photon numbers and the results
of the FWHM are summarized in Fig. 2(c).

We also estimate the sensitivity from the measurements
and the results for two different mean photon numbers are
presented by the insets of Fig. 2. These results demonstrate
that the measurements possess a phase sensitivity
very close to the SNL (dashed line) for certain phases.
In Fig. 2(d) we present a summary of the optimal phase
sensitivities for several different mean photon numbers and
compare it to the SNL (dashed curve).

As we have now seen, binary binning of quadrature
measurements leads to a narrowing of the interference
fringe. However, the number of fringes in a 2π period
remains unchanged as opposed to interferometry with
NOON states where the number of fringes increases
with the photon number. It is, however, also possible
with coherent states to increase the number of fringes in
a period by employing a multiple binning approach:
Instead of dividing the measurement results in two differ-
ent intervals, we divide them into multiple intervals con-
sisting of equidistant bins with length $2a$. This is described
by the projectors

$$\hat{\Pi}_k = \int_{b_k-a}^{b_k+a} |p'\rangle\langle p'| dp' \qquad \hat{\Pi}_{n+1} = \hat{I} - \sum_{k=1}^{n} \hat{\Pi}_k. \quad (7)$$

By setting the eigenvalues $\lambda_k = 1/\text{erf}(\sqrt{2}a)$ for $k \in$
$\{1, \ldots, n\}$ and $\lambda_{n+1} = 0$, we find the resulting response
function

$$\langle\hat{\Pi}\rangle = \frac{1}{2\,\text{erf}(\sqrt{2}a)} \sum_{k=1}^{n+1} \{\text{erf}[\sqrt{2}(g_- - b_k)] \\ + \text{erf}[\sqrt{2}(g_+ + b_k)]\} \quad (8)$$

where b_k is the central position of the intervals on the
p-quadrature line. If the distance between the intervals is
$b > 2a$, the projectors are orthogonal and we can straight-
forwardly find the quantity

$$\langle \Delta \hat{\Pi}^2 \rangle = \langle \hat{\Pi} \rangle \left(\frac{1}{\mathrm{erf}(\sqrt{2}a)} - \langle \hat{\Pi} \rangle \right) \qquad (9)$$

and thus the sensitivity $\Delta \phi$.

An example is shown in Fig. 3 for $a = 1/2$ and 8 fringes. The multiple fringe approach will, however, give rise to a slightly lower visibility of the interference fringes, thus rendering a trade-off between the number of fringes within a period and the visibility of the resulting pattern for a given average photon number. It is however possible to recover the near unity visibility by increasing the number of photons as illustrated in Fig. 3(c). This means that the phase sensitivity of the multifringe approach operates at the SNL (like the two bin approach) as long as the number of fringes is adjusted according to the mean number of photons.

For a fixed number of photons N, the number of fringes M depends on the choice of the parameter b as well as on the required visibility. For a given set of N, M, and a there is an optimal value of b that maximizes the visibility. Figure 3(c) reports two examples of the number of fringes as a function of the number of photons for two different visibilities. In this example, for each N, b has been chosen such as to maximize M and to keep the visibility above 95% or above 90%. It is clear that at higher visibility the number of fringes for a given N decrease. The points in the figure are extracted by numerical calculation and the curves are fits that scale as $M \propto \sqrt{N}$.

In the above investigations we have considered only the measurement of the phase quadrature among all other quadratures. For the binary binning approach, this is indeed the optimal quadrature measurement [for the input state considered in Fig. 1(a)] although superresolution with reduced quality can be also obtained for any other quadrature measurement. This is clearly seen from the results of the multiple-bining approach in Fig. 3 which shows that the fringes are narrowest at $\phi = 0$ and broadest at $\phi = \pi/2$ effectively corresponding to a phase and an amplitude quadrature measurement, respectively. The fact that superresolution can be obtained for any quadrature measurement suggests that we may relax the stringent phase reference in our homodyne detector thus measuring a random quadrature and thereby attaining superresolution with a simplified strategy.

In contrast to previous superresolution schemes based on NOON states or photon counters, the measurement presented here is intrinsically deterministic. It means that we keep every single measurement outcome and do not perform a postselection of the outcomes to extract the desired superresolving feature as done in previous implementations [7–10,20,22]. Due to this common post selection procedure (which significantly reduces the number of available resource states), all these experiments exhibit a phase sensitivity that is lower than the one obtained here if the actual number of photons passing through the phase sample is taken into account. A more promising approach to deterministically beat the SNL (and eventually reaching
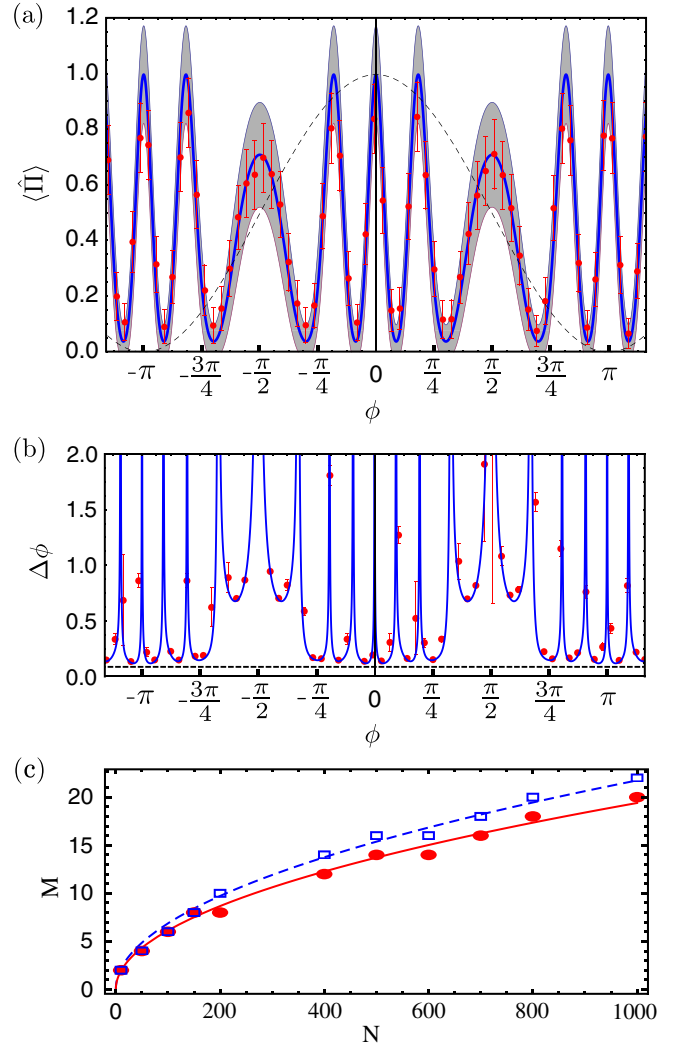

FIG. 3 (color online). Results for the multiple binning approach. (a) Response function with 8 fringes per period obtained by binning the measurement outcomes along 5 intervals for a coherent state with $N = 139$. The central points of these intervals are located at $p = b \cdot k$ where $k \in [-2, -1, 0, 1, 2]$ and $b = 3.17$. The average fidelity of all fringes within a period is 95%. The data (red dots) fit well with theory (blue line) and the uncertainty for each point lies inside the theoretically predicted uncertainty, represented by the shaded area. The interference fringe corresponding to the Rayleigh limited approach is shown by the dashed curve. (b) Phase sensitivity for the multiple binning approach associated with the experimental results (dots) and the theory (solid curve). Near the SNL, performance (represented by the dashed line) is obtained for several phases. (c) Plot of the number of fringes M for which the visibility is larger than 0.95 (red solid trace and dots) and 0.90 (blue dashed trace and squares) as a function of the average photon number, N, of the coherent state. The dots and squares correspond to numerical estimates whereas the curves are theoretical fits.

the Heisenberg Limit) is the one based on single photons in a multiple-pass interferometer although its performance will be ultimately limited by the extended time of flight of the photons [15,16].

Using a very simple setup based on coherent states and a high-efficiency homodyne detector, we have demonstrated a narrowing of the interference fringes of an interferometer beyond what is possible with conventional interferometers. In contrast to previous implementations of superresolution with coherent states, the proposed scheme is deterministic and it attains a phase sensitivity at the shot noise limit. Both the phase resolution and the phase sensitivity were found to scale inversely with the coherent state amplitude.

---

*Present address: ICFO, The Institute of Photonic Sciences, Mediterranean Technology Park, 08860 Castelldefels, Spain.

[1] M. Born and E. Wolf, *Principle of Optics* (Cambridge University Press, Cambridge, England, 1999).

[2] A. N. Boto, P. Kok, D. Abrams, S. Braunstein, C. Williams, and J. Dowling, Phys. Rev. Lett. **85**, 2733 (2000).

[3] D. Leibfried *et al.*, Nature (London) **438**, 639 (2005).

[4] J. A. Jones, S. D. Karlen, J. Fitzsimons, A. Ardavan, S. C. Benjamin, G. A. D. Briggs, and J. J. L. Morton, Science **324**, 1166 (2009).

[5] Y.-A. Chen, X.-H. Bao, Z.-S. Yuan, S. Chen, B. Zhao, and J.-W. Pan, Phys. Rev. Lett. **104**, 043601 (2010).

[6] J. G. Rarity, P. R. Tapster, E. Jakeman, T. Larchuk, R. A. Campos, M. C. Teich, and B. E. A. Saleh, Phys. Rev. Lett. **65**, 1348 (1990).

[7] M. W. Mitchell, J. S. Lundeen, and A. M. Steinberg, Nature (London) **429**, 161 (2004).

[8] P. Walther, J.-W. Pan, M. Aspelmeyer, R. Ursin, S. Gasparoni, and A. Zeilinger, Nature (London) **429**, 158 (2004).

[9] T. Nagata, R. Okamoto, J. L. O'Brien, K. Sasaki, and S. Takeuchi, Science **316**, 726 (2007).

[10] I. Afek, O. Ambar, and Y. Silberberg, Science **328**, 879 (2010).

[11] V. Giovanetti, S. Lloyd, and L. Maccone, Nat. Photonics **5**, 222 (2011).

[12] J. Fiurášek, Phys. Rev. A **65**, 053818 (2002).

[13] M. A. Rubin and S. Kaushik, Phys. Rev. A **75**, 053805 (2007).

[14] U. Dorner, R. Demkowicz-Dobrzanski, B. Smith, J. Lundeen, W. Wasilewski, K. Banaszek, and I. Walmsley, Phys. Rev. Lett. **102**, 040403 (2009).

[15] B. L. Higgins, D. W. Berry, S. D. Bartlett, H. M. Wiseman, and G. J. Pryde, Nature (London) **450**, 393 (2007).

[16] B. L. Higgins, D. W. Berry, S. D. Bartlett, M. W. Mitchell, H. M. Wiseman, and G. J. Pryde, New J. Phys. **11**, 073023 (2009).

[17] K. L. Pregnell and D. T. Pegg, J. Mod. Opt. **51**, 1613 (2004).

[18] S. J. Bentley and R. W. Boyd, Opt. Express **12**, 5735 (2004).

[19] G. Khoury, H. Eisenberg, E. Fonseca, and D. Bouwmeester, Phys. Rev. Lett. **96**, 203601 (2006).

[20] K. J. Resch, K. Pregnell, R. Prevedel, A. Gilchrist, G. Pryde, J. O'Brien, and A. White, Phys. Rev. Lett. **98**, 223601 (2007).

[21] Y. Gao, P. M. Anisimov, C. F. Wildfeuer, J. Luine, H. Lee, and J. P. Dowling, J. Opt. Soc. Am. B **27**, A170 (2010).

[22] F. Guerrieri, L. Maccone, F. N. C. Wong, J. H. Shapiro, S. Tisa, and F. Zappa, Phys. Rev. Lett. **105**, 163602 (2010).

[23] C. Kothe, G. Bjork, and M. Bourennane, Phys. Rev. A **81**, 063836 (2010).

[24] H. Shin, K.-W.-C. Chan, H. J. Chang, and R. W. Boyd, Phys. Rev. Lett. **107**, 083603 (2011).

[25] N. Plick William, P. M Anisimov, J. P Dowling, H. Lee, and G. S Agarwal, New J. Phys. **12**, 113025 (2010).